END

FILMED

DTIC

MICROCOPY RESOLUTION TEST CHART

NATIONAL BUREAU OF STANDARDS-1963-A

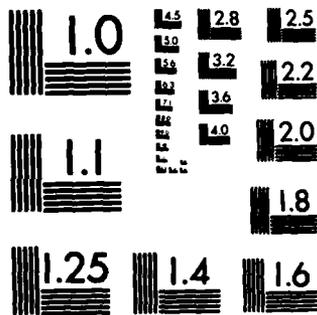(12)

OFFICE OF NAVAL RESEARCH

Contract N00014-83-K-0470

Task No. NR 359-718

TECHNICAL REPORT NO. 34

Modulated Surface Vibrational Spectroscopies at
Electrode/Electrolyte Interfaces

By

Stanley Pons
Alan Bewick

Prepared for Publication in

Naval Research Reviews

University of Utah
Department of Chemistry
Salt Lake City, Utah   84112

DTIC
ELECTE
DEC 2 1 1984
B

November 28, 1984

AD-A148 665

DTIC FILE COPY

84   12   12   043

REPORT DOCUMENTATION PAGE		READ INSTRUCTIONS BEFORE COMPLETING FORM
1. REPORT NUMBER 34	2. GOVT ACCESSION NO. AD-A148665	3. RECIPIENT'S CATALOG NUMBER
4. TITLE (and Subtitle) Modulated Surface Vibrational Spectroscopies at Electrode/Electrolyte Interfaces		5. TYPE OF REPORT & PERIOD COVERED Technical Report # 34
		6. PERFORMING ORG. REPORT NUMBER
7. AUTHOR(s) Stanley Pons and Alan Bewick		8. CONTRACT OR GRANT NUMBER(s) N00014-83-K-0470
9. PERFORMING ORGANIZATION NAME AND ADDRESS University of Utah Department of Chemistry Salt Lake City, UT 84112		10. PROGRAM ELEMENT, PROJECT, TASK AREA & WORK UNIT NUMBERS Task No. NR 359-718
11. CONTROLLING OFFICE NAME AND ADDRESS Office of Naval Research Chemistry Program - Chemistry Code 472 Arlington, Virginia 22217		12. REPORT DATE November 28, 1984
		13. NUMBER OF PAGES 31
14. MONITORING AGENCY NAME & ADDRESS(if different from Controlling Office)		15. SECURITY CLASS. (of this report) Unclassified
		15a. DECLASSIFICATION/DOWNGRADING SCHEDULE

16. DISTRIBUTION STATEMENT (of this Report)

This document has been approved for public release and sale; its distribution unlimited.

17. DISTRIBUTION STATEMENT (of the abstract entered in Block 20, if different from Report)

18. SUPPLEMENTARY NOTES

19. KEY WORDS (Continue on reverse side if necessary and identify by block number)

Infrared Spectroelectrochemistry

20. ABSTRACT (Continue on reverse side if necessary and identify by block number)

DD, FORM 1473 EDITION OF 1 NOV 65 IS OBSOLETE
S/N 0102-LF-014-6601

MODULATED SURFACE VIBRATIONAL

SPECTROSCOPIES AT ELECTRODE/ELECTROLYTE INTERFACES

Stanley Pons
Department of Chemistry
University of Utah
Salt Lake City, UT   84112

and

Alan Bewick
Department of Chemistry
University of Southampton
Southampton, England   S09 5NH

INTRODUCTION

Reactions at the solid-liquid and solid-gas interface have become the topic of considerable attention in the last-ten years due to their controlling influence in energy-producing and catalytic devices. The complete study of these reactions can only be accomplished if something about the energetics and structure of the reactants, intermediates, and products at the interface are known, in addition to the kinetic parameters. At this point, it becomes more realistic to attempt designing custom devices for specific chemical reactions. Thus in addition to being able to study the fundamental principles involved in the surface processes, there are great practical reasons to undertake these often difficult studies.

Rapid progress in this area will require collaboration between electrochemists on the one hand and materials scientists together with high vacuum surface scientists on the other. The molecular specific information now becoming available to the electrochemist from the range of techniques outlined in ths article provide the vital data necessary to establish the channel of communication between the various disciplines; the electrochemist can now provide the materials scientist with the information he requires in order to model new electrocatalysts and other materials for the energy conversion area; this is one of the major immediate benefits arising from the applications of the techniques.

Some of the classically important electrochemical surface reactions which are still being intensely investigated are the redox chemistry of hydrogen at metal electrodes, metal corrosion reactions, adsorbed intermediates in the catalytic oxidation of small molecules at noble metal electrodes (fuel cells), the effects of adsorbed or chemically-bound structures on the surfaces of electrodes on the course and efficiency of solar energy conversion devices,

the fundamental properties of semiconductor based energy conversion devices, and the investigation of reactions at the surfaces of battery electrodes.

In this report, we will discuss the applicability of a new infrared vibrational probe to studies of the structure and orientations of molecular species at or near the electrode-solution interface and the dynamics of adsorption/desorption processes. Such studies have been virtually impossible with available instrumentation in the past due to the extremely large absorbance by the solvent/electrolyte system. Early investigations on electrochemical systems were thus attempted primarily with internal reflectance methods that did not require that the radiation pass through the bulk solvent/electrolyte system (1) (Figure 1a). This method is limited, however, due to the few choices of infrared-transport electrode materials (semiconducting materials or very thin metal films on insulating transparent salts and polymers) in addition to more stringent cell designs and electrode geometries. In 1979, we demonstrated that in fact it was possible to reflect the light externally from the electrode through the strongly absorbing solution and still obtain an infrared spectrum of very small numbers of absorbers near the electrode surface (2) (Figure 1b). This was made possible by a number of factors, including the adaptation of spectroelectrochemical potential modulation techniques that had already been developed for the UV/VIS regions (3), the use of thin layer electrochemical cells to reduce the effective path length of the strongly absorbing solution, and the development of more sensitive infrared spectrometers in our labs and in the commercial sector. The methods have been termed electromodulated infrared reflectance spectroscopy (EMIRS) and subtractively normalized interfacial Fourier transform infrared spectroscopy (SNIFTIRS) (4-8). Refinements to these techniques in the last five years have led to methodology which allows the

study of sub-monolayer amounts of adsorbed material at electrode surfaces in situ to the electrochemical experiment in short periods of time. In addition, studies of chemical reactions near the surface involving electrogenerated species are also facilitated by the method, as are studies of the electrical double layer. We will present a few examples of each type of study following a brief description of the principles of infrared absorption of oscillators at metal surfaces, and some details concerning the experimental apparatus and method.

INTERACTION OF INFRARED RADIATION WITH ADSORBED SPECIES

The interaction of electromagnetic radiation with the surface of a highly reflecting plane metal surface depends strongly on the polarization of the radiation with respect to the incidence plane. The intensity of the electric field vector at the surface is a measure of the intensity of the radiation at the surface, and is thus a measure of the energy available to interact with adsorbed oscillators at the surface. The angle of incidence of the radiation with respect to the surface also affects the field intensity of the radiation, and affects the various polarizations differently. The relation between the strength of the electric field vector, the polarization of the radiation and the angle of incidence is shown diagramatically in Figure 2. It is seen that the electric field strengths are largest at high angles of incidence to the surface normal, and that it is only the component of radiation that is polarized parallel to the incidence plane (p-polarized) that has field strength at the surface at any angle of incidence. Radiation polarized perpendicular to the incidence plane (s-polarized) is thus "blind" to absorbers present in regions very near the metal surface. Absorption of infrared radiation by a molecule occurs anytime there is (a) an accompanying

change in magnitude of an oscillating dipole moment in the molecule, and, (b) a component of the electric field of the radiation that is parallel to the normal coordinate axis of that oscillating dipole. In solution, all infrared-allowed transitions will be observed at any polarization due to the random orientation of the oscillators in the optical path. On the other hand, surface confined oscillators will have various normal coordinate dipole axes fixed with respect to the incident radiation. Since the surface also affects the magnitude of the radiation, the intensity of interaction will depend on the polarization state and the orientation of the adsorbed species. These optical properties give rise then to three important consequences to infrared spectroelectrochemistry. (i) S-polarized radiation is of no use in detection of species at or near the interface, and is usually eliminated by various means in the experiments described here before reaching the detector. (ii) Since none of the infrared radiation is able to give rise to a tangential field at the surface, not all of the normally infrared active vibrational modes of a molecule are observable in the adsorbed state; those not having a finite value of $(\partial\mu/\partial Q)$ (the dipole moment derivative with respect to the normal coordinate under consideration) normal to the surface are invisible to the radiation. This is known as the vibrational surface selection rule. The magnitude of an absorption coefficient for any infrared transition is proportional to the square of the magnitude of the electric field of the radiation at the dipole and the magnitude of the dipole derivative given above. If the direction of the dipole derivative (it is a vector quantity) is tilted at some angle ϕ to the surface normal, then the intensity of the absorbance will vary as $\cos^2\phi$. Thus the relative intensities of bands from the normal mode vibrations enable the orientation of the molecule to be deduced. (iii) It is also clear from the foregoing discussion that p-

polarized radiation is able to interact with all species in the spectrometer optical path and all species in the reflectance cell. S-polarized radiation behaves the same except it does not interact with species close to the metal electrode surface. Thus, the difference between two beams, one p- and one s-polarized, and of equal intensity, is simply the absorbance of those molecules near the surface, all ambient effects having been cancelled. This point is the basis for polarization modulation techniques that are also used in conjunction with the basic potential modulation schemes described herein to acquire additional information (4-6).

In addition to the optical radiation electric field interaction with oscillating dipoles, other interactions with external electric fields are likely, and we have reported observing some of these interactions recently. The perturbation of vibrational spectra by intense electromagnetic fields has been known for many years (9-12). The effect of a strong electric field on the frequency and/or frequency splitting of a rotating molecule (the Stark effect) has been studied in the gas phase and in condensed systems (13-16). These systems have traditionally been studied by developing the electric field with two parallel electrodes across a dielectric containing the species of interest. In addition, Devlin, et. al. (18) have discussed the possibility of charge transfer interactions causing activation and perturbation of certain vibrational modes, and have discussed the participation of metal surfaces to this charge transfer mechanism. In this case, generally weaker external electromagnetic fields [crystal lattices (19), "uncharged" metal surfaces (20), dimers (21), etc.] are required to cause further induced dipole effects. With regard to the former, strong interactions, Palik, et. al. (13,14) have observed the Stark effect in several systems, but have pointed out that the intensity changes as originally predicted by Condon (9) are the

most predominant effects in the field induced infrared spectra of the systems studied. Condon pointed out that the induced dipole moment in the direction of the polarization of the electromagnetic radiation by a strong external electric field will be proportional to the square of the mean field intensity. We have observed (4,21-24,34), using both EMIRS and SNIFTIRS, electric field dependence in the intensity of vibrational bands that should not be active in the domain of Z-field surface selection rule predictions discussed above, and thus we attribute these to the inducing of dipole moments by the strong electric field produced at the electrode/electrolyte solution interface; using the broadest definition, these are electrochemical manifestations of the Stark effect. In an experiment where the electromagnetic radiation is polarized in a direction ε, the induced dipole moment tensor in that direction by an externally applied electric field is simply:

$$P_\ell = \alpha_\ell E_\ell$$

where α_ℓ is the element of the polarizability tensor in the direction of the polarization of the infrared radiation, and E_ℓ is the component of the applied electric field in the same direction. The integrated Einstein absorption coefficient for the band is given by

$$B = \frac{2\pi^2 \nu T}{\varepsilon_0 \hbar c} \, |P_{fi}|^2$$

where ν is the optical frequency of the infrared transition, h is Planck's constant, c is the velocity of light, T is the number of absorbing dipoles per unit cross sectional area in the radiation path, ϵ_0 is the permittivity of free space, and P_{fi} is the transition dipole matrix element. In the presence of an external magentic field, the dipole moment tensor can be expressed in terms of the value of the permanent dipole moment and the induced value. We have shown that (24) this leads to:

$$|P_{fi}| = \langle \Psi_{\nu_f} |P_0'| \Psi_{\nu_i} \rangle + E\langle \Psi_{\nu_f} |\alpha'| \Psi_{\nu_i} \rangle$$

where P_0' and α' correspond to the change in the permanent dipole moment and polarizability with respect to a normal coordinate, respectively. The integrated absorption coefficient becomes

$$B = \frac{2\pi^2 \nu T}{\epsilon_0\ hc} |\langle \Psi_{\nu_f} |P_0'| \Psi_{\nu_i} \rangle + E\langle \Psi_{\nu_f} |\alpha'| \Psi_{\nu_i} \rangle|^2$$

We have calculated the expected values for the induced absorption coefficient for the C=C symmetric stretch for several molecules adsorbed flat on a metal electrode and for CO adsorbed perpendicular to the metal electrode, both in the presence and absence of an electric field. We assume close-packed simple monolayer coverage of the species on a planar 1 cm^2 surface. Since the matrix elements $\langle \Psi_{\nu_f} |\alpha'| \Psi_{\nu_i} \rangle$ are not tabulated for molecules larger than diatomic, we have estimated the change in polarizability with normal

coordinate for the given transition to be of the same order of magnitude as the fixed polarizability normal to the molecular axis. This approximation is the upper bound value of the matrix element; the actual value will normally be somewhat smaller. The results of the calculation are given in the table. These values reflect the very strong dependence of the effect on the nature of the molecule.

$$B/10^{-3} \, cm^{-1} \, (Ag \, Mode, \, see \, text)$$

Electric Field Strength V/m	CO	C_2H_4	Napthalene	Anthracene	TCNQ⁻
10^7	4.2				
10^8	4.5		0.056	0.1	1.5
10^9	7.5	0.6	5.6	11	150
2×10^9	12	2.4	22	44	580
5×10^9	30	15	140	280	3,600
8×10^9	56	40	350	710	9,300
10^{10}	79	62	560	1,100	14,500

Examples of the effect will be discussed later in the report.

Experimental Details

The cell for performing the EMIRS and SNIFTIRS experiments is shown in Figure 3. The working electrode is a polished mirror of the desired material and is mounted on the end of a glass syringe barrel or is attached to the end

of a metal rod that is tightly sheathed in a Kel-F sleeve so that only the working face is subjected to the electrolyte solution. This assembly is fitted into a matching glass barrel which is an integral part of the cell body, such that the face of the electrode is made to contact an optically transparent window at the opposite end of the cell. A thin layer of solution through which the optical beam is made to pass is thus trapped between the electrode face and the optical window. This layer is typically 1 to 100 micrometers thick, depending on the application. The cell is equipped with a Luggin capillary reference probe, and a wire loop secondary electrode through which the working electrode assembly passes. The three electrode assembly allows accurate potential control to be exerted on the working electrode by conventional electrochemical potentiostat equipment. A variety of infrared optical windows may be used on the cell depending on the particular application. Polyethylene is usually used in the far-infrared region, whereas silicon, calcium fluoride, and various IRTRAN materials are common for the mid-infrared region. Flat windows are used in many cases, but prismatic types reduce reflection losses at the atmosphere/window interface allowing more of the radiation to be utilized at the solution/electrode interface. More details on the cell and experimental setup have been published (4-6). In both EMIRS and SNIFTIRS, the cell is mounted in a spectrometer sampling area, and the radiation beam is made to reflect from the mirror electrode after passing through the solution layer. In EMIRS, the reflected beam is focussed carefully onto the entrance slit of a high-throughput infrared monochromator, and after polarization, dispersion, and filtering of the radiation, is focussed onto the active area of a sensitive detector. The potential of the electrode is then modulated between two values at which the electrochemistry is different. The population or form of the various species at the interface

is also modulated at the same frequency, and therefore the infrared radiation intensity as well. The intensity change at this modulation frequency is amplified and measured by synchronous demodulation of the detector output signal using a lock-in amplifier. This signal is stored for further processing in an integrated control computer system. The design of these high throughput instruments have been discussed elsewhere in detail (5,6). Presently, one such instrument, the EMIRS III spectrometer, is commercially available.

Further processing of the data requires normalizing the difference signal just discussed to the background throughput which is obtained by conventional chopping of the beam while scanning the spectrum. The final value may be represented as $\Delta R/R$, or the difference in reflectance at the two potentials divided by the total reflectance at one of the potential values. For very low values of the difference signal, the resulting ratio is equivalent to true absorbance. Due to the way in which the experiment is performed, the spectrum is of the difference type and will have bands pointing in one direction that will be due to the absorbing species at one of the potential limits, and in the opposite direction for the related species at the other potential limit. The technique is highly sensitive, and typically yields a noise level of only 0.00001 absorbance units through an aqueous sample in a single scan. Thus the averaging of 100 such scans gives a sensitivity of 0.000001 absorbance units which is sufficient for the study of surface coverages of much less than one monolayer.

SNIFTIRS is the equivalent technique performed on an interferometric Fourier transform infrared spectrometer. Sensitivity in this case is accomplished by the throughput and multiplex advantages of such instruments; digital signal averaging of the more intense signals at the detector allows

many more spectra to be taken in unit time than the dispersive instrument.
The result is similar sensitivity in both instruments, if care is taken to
optimize all of the relevant parameters such as throughput, detector
sensitivity, cell design and alignment, etc. The choice of a suitable Fourier
transform spectrometer has been discussed (4-6). In SNIFTIRS, interferograms
are recorded at each electrode potential limit individually, coadded into two
separate digital files repeatedly until the required signal-to-noise level is
attained, and ratioed against each other after suitable correction for
radiation reflection from the front window surface. The resulting spectra are
equivalent to the $\Delta R/R$ results discussed above.

Examples

There are three basic types of research that have been undertaken thus
far. One has been the study of solution soluble radical ion intermediates
electrogenerated at the interface from organic substrates. The thin layer
cell described is ideal for the preparation of such species. In the SNIFTIRS
method, spectra are first recorded at a potential value where the substrate is
stable. The electrode potential is then stepped to a value where all of the
organic substrate in the thin layer of solution is rapidly converted to the
radical ion form. Spectra are then recorded again of the interfacial area,
and the two sets of data treated as described above. The second type of study
has been the investigation of the structure and reorganization of the double
layer region as the potential of the electrode is changed. The third line of
research has concentrated on the important practical areas mentioned in the
introduction: that of the structure and reactions of adsorbates at metal
surfaces, and the effect of surface adsorbed species on heterogeneous
catalysis at electrode surfaces.

The SHIFTIRS difference spectrum of the benzophenone ketyl anion radical electrogenerated in acetonitrile at a platinum mirror electrode is shown in Figure 4. The base potential where substrate is stable was -1.75 V and the second potential, where radical anion is generated, was -2.50 V vs. the Ag/Ag$^+$ (0.01 M to 0.2 M tetra-n-butylammonium tetrafluoroborate) reference electrode. The bands extending upward correspond to predominate species at the base potential (that of the substrate) while the bands extending downwards correspond to predominate species at the second potential (that of the ion radical). For reference, a conventional transmission spectrum of the benzophenone substrate is included in the figure. Each of the ketyl ion radical bands observed are in excellent agreement, both in frequency and intensity, with those reported by other workers. For a reversible electron transfer reaction, it can be shown that under conditions of semi-infinite linear diffusion (which should be the case in the relatively thick solution layer) the normalized reflectance should increase linearly with $\tau^{1/2}$ where τ is the electrolysis time. Using a rapid scan mode available on most Fourier transform spectrometers to obtain interferograms at 12.5 ms intervals throughout the 1.5 s duration of the pulses at the second potential, this linear relationship was verified for several of the bands in the spectrum. In this type of experiment, it is important to ensure that the thin layer contents are reproducibly returned to rest conditions after each excursion to the electrolysis potential. Thus with reasonable care, quantitative time resolved spectrochemistry is possible using this technique.

The difference spectrum of benzophenone/benzophenone ketyl shows a large wavenumber shift in the C=O stretching band (1661 cm^{-1} in the substrate and 1555 cm^{-1} in the ketyl anion). Strong localization of the unpaired electron at the C=O moiety is responsible for this shift. A general red shifting of

the ring modes in going from the neutral molecule to the ketyl anion has been discussed previously (25). When this same system is studied using only a very thin layer of solution (less than 1 µm) a larger percentage of the difference spectrum can be attributed to surface related phenomena. Indeed, a complex interaction is indicated by the appearance of several new bands at 1340 cm^{-1}, 1464 cm^{-1} and 2120 cm^{-1}. The intensities of these bands compared to those from the anion radical in solution and the dependence upon solution thickness indicate that they are due to adsorbed intermediates probably enhanced by the Stark interactions mentioned above.

Spectra have been obtained from the potential dependent population of species in the double layer formed at a Pt electrode in contact with a simple base electrolyte in acetonitrile (26). Figure 5 shows the potential dependence of the spectra from a 0.10 M tetrabutylammonium tetrafluoroborate (TBAF) solution of thickness about 1 µm. The base potential to which the spectra are references is -0.50 V vs. the Ag/Ag$^+$ 0.01 M in the same electrolyte solution. The solution was carefully dried before the measurements, the estimated water content being less than 10^{-4} M. Marked .changes are evident at the 3000 cm^{-1}, 2350 cm^{-1}, 1400 cm^{-1} and 1100 cm^{-1} spectral regions. Figure 6 shows the same system run under the same conditions after the solution was made 0.10 M in water. Additional absorbance changes are evident at the 3200-3700 cm^{-1} and the 1630 cm^{-1} regions.

Certain aspects of the spectra are readily explained: the increasing adsorption of acetonitrile at the electrode with increasing positive potential is evident from the progressively increasing intensity at the upper potential of the 2350 cm^{-1} band. This band is strongly blue shifted frm the bulk acetonitrile band by the perturbation of the molecule due to adsorption (bulk acetonitrile has a C $\equiv$ N fundamental vibrational mode at 2200 cm^{-1}); the

increasing amount of anion in the double layer is indicated by the dominant downward extending bands (at high positive potentials) at 1060 cm^{-1} (tetrafluoroborate). The upward extending fine structure on the C $\equiv$ N band between 2000 cm^{-1} and 2400 cm^{-1} is due to decreased absorption by bulk acetonitrile at the expense of adsorbed acetonitrile.

The complex structure between 3300 cm^{-1} and 3600 cm^{-1} and that near 1630 cm^{-1} which appear when water is added to the system can be attributed to fundamental modes of water in different environments. The broad band at 3350 cm^{-1} corresponds to extensively hydrogen bonded water, possibly associated with the anion, and it is noted that the intensity increases as more anion is drawn into the double layer. The sharper bands of opposite sign at 3625 cm^{-1}, 3550 cm^{-1}, and 1625 cm^{-1} appear to originate from water that is not so strongly perturbed by hydrogen bonding. The species responsible is probably the symmetrically bonded complex between two acetonitrile molecules and one water molecule, a species that has been well characterized previously (27). The ν_1, ν_2 and ν_3 modes for this species are at the wavenumbers listed above. The intensities of these bands are potential dependent, and are seen to decrease at the more positive potentials indicating a decreasing population of this species at these potentials.

The above assignments lead to the following general explanation of the spectra in terms of the dependence on the electrode potential of the relative amounts of each of the species in the optical path. As the electrode potential is made more positive, additional anion is required in the double layer to balance the charge. Increased amounts of acetonitrile are adsorbed at the surface as well. Migration of additional anion into the optical path from the bulk electrolyte increases the total amount of anion in the path. The net increase of these two species thus accounts for the increase in

intensities of the appropriate bands. As a result, bulk acetonitrile and its associated water are forced out of the region, and the intensities are seen to be displaced in the upward direction (less absorbance) at the more positive potentials.

Changes in the C-H stretch of the cation are also observed. This band is in the 2900 cm^{-1} - 3050 cm^{-1} region. The major portion of this band is extending upwards which corresponds to a net decrease in the amount of cation at the more positive potentials. Changes in bandshape are indicated by the bands extending in the opposite direction. This example shows the considerable amount of detailed information on the composition of the double layer that becomes accessible by comparatively simple experiments. Although these first measurements have not been used to derive quantitative information on the amounts of the various species observed in the diffuse double layer or adsorbed on the electrode, it will certainly be possible to make quantitative deductions; initially this will require careful sets of measurements on selected model systems in order to establish confidence in the calibration of band intensities for species close to or on the metal surface.

The reduction of water a metal electrodes, the hydrogen evolution reaction, and its reverse reaction, the oxidation of hydrogen, are electrocatalytic reactions with adsorbed hydrogen atoms as intermediates. On many metals, particularly those of the platinum group, there may be several kinds of hydrogen on, or partially in, the surface. On Pt and Rh electrodes, at potentials just positive of hydrogen evolution, the surface is covered by at least two types of adsorbed species. At more positive potentials the weakly adsorbed species desorbs, leaving only strongly adsorbed hydrogen. At still more positive potentials this is also oxidized off the surface. The region of potential between that of adsorbed hydrogen and that of platinum

surface oxide formation is known as the double layer region. These systems have previously been investigated by UV/visible spectroelectrochemistry (28-29). Surface EMIRS spectra have now been obtained for Pt (30) and Rh (31) electrodes in aqueous acid solutions.

Modulation within the double layer region of potential gave only a small and featureless change of reflectivity from the electroreflectance effect and from double layer reorganization involving species not absorbing strongly in the spectral range covered.

Modulation into the potential range of strongly bound hydrogen also gave a featureless spectrum, but with a 30-fold increase in the reflectivity change, similar to the optical effect observed for this species in the UV/visible-region. It has been suggested (28) that strongly adsorbed hydrogen consists of a proton buried just inside the metal surface with its electron in the conduction band of the metal. The increase in the number of conduction electrons on adsorption of the strongly bound species would then be responsible for the increase in reflectivity.

Modulation into the potential range weakly bound hydrogen, however, gave several absorption bands superimposed on the baseline shift from the strongly bound species also present. These bands were all at the same wavelengths as those for the vibrational modes of water, and all had the same sign, corresponding to an increase in the amount of water in the interface when weakly adsorbed hydrogen was formed. Similar experiments with H_2O/D_2O gave up to nine bands (from H_2O, HDO and D_2O species) the positions of which were used to confirm the band assignment. H_2O/D_2O solvent mixtures were used for two reasons. Firstly, to increase the energy transmitted through the solution in the spectral regions covering the water absorption bands and hence to increase the sensitivity in these difficult regions. Secondly, the isotopic shifts of

the vibration frequencies helped with the assignment of some of the combination bands. The relative intensities of those observed bands were used to deduce the orientation of the water interacting with the weakly adsorbed hydrogen by applying the surface selection rule to a series of models. The only model which fitted the data is shown in Figure 7a. It consists of oriented dimer units bonded to hydrogen atoms on the surface, the dimer units also being hydrogen bonded to water further away from the surface. Further evidence for the strong interaction of the weakly adsorbed hydrogen with water is provided by the absence of a prominent band from the Pt-H stretch. The reference state used in determining the structure of the interacting water, which is the state of the surface in the double layer region, is also shown in Figure 7b. It is assumed to consist of a layer of water molecules, each with one lone pair orbital normal to the surface, so that the molecular dipoles are at a lower angle to the surface than is the case for the water molecules bonded to the adsorbed hydrogen. Then a modulating from the double layer region to the potential region of weakly adsorbed hydrogen the water bands increase in intensity due to the surface selection rule, giving negative-going bands, on adsorption. This orientation for the reference state also fits other electrochemical data (32).

To date, fuel cells have found only limited applications in energy conversion areas in spite of their great potential benefits. The major obstacle has been the development of cheap and efficient electrocatalysts, particularly for systems directly utilizing a primary organic fuel without initial reforming. This is a prime example of an area requiring interdisciplinary collaboration of the type mentioned earlier in this article. One of the first applications of the EMIRS technique was in the detection and identification of the major poisoning species formed on platinum

group metal electrocatalysts during the electrocatalytic oxidation of fuels such as methanol, formaldehyde, or formic acid. Figure 8 gives examples of the spectra obtained from a poisoned electrode for the system platinum/formaldehyde/sulfuric acid (33). The two bipolar bands clearly visible in Figure 8A are from the CO stretch vibrations of two different strongly adsorbed CO poisons. The higher wavenumber band is from $CO_{(ADS)}$ bonded directly on top of a surface platinum atom and the lower wavenumber band is from the same molecular species bound in a higher coordination site between surface metal atoms. The addition of a partial monolayer of lead atoms to the surface can be seen, Figure 8B, to inhibit the formation of these poisons, particularly the latter, and this effect coincides with increased catalytic activity. The proper identification of the poisoning species is of considerable importance since it had been wrongly assumed from the analysis of indirect electrochemical evidence that it was $COH(_{ADS})$. In this example, the bipolar shape of the bands arises from the considerable shift of the IR absorption bands with electrode potential for these species. This effect is in itself very interesting because of the information it gives on the nature of the bonding between the metal and $CO_{(ADS)}$.

One example of the Stark activation of a totally symmetric A_g ring mode is clearly seen in Figure 9. The experiment was by SNIFTIRS in acetonitrile solvent, from -1.5 to -2.5 V vs Ag/Ag^+ reference. The intensity (B) of the band is about 1% of the value given in the table above for an assumed field strength of 10^8 V/M. On the other hand, the upper bound value given in the table for CO predicts a 70% increase in the band intensity on going from zero field to 10^9 V M^{-1}. Since the actual effect is likely to be closer to 1% of the upper bound, we conclude that its detection will be very difficult. For ethylene, we estimate that a sensitivity of 5×10^{-5} absorbance would be

required at a field strength of 10^9 V M^{-1} and thus it should be measurable. We also point out that the electrochemically activated Stark effect (TEASE) might be used as a probe for measuring electric field intensities in the electrical double layer. Adsorbed species will also be under the influence of a variety of fields arising from other sources such as surface adatoms, impurities, and surface defects. We also mention that the above treatment neglects quadrapole and higher expansion terms, and magnetic effects, which although normally small compared to the dipole term, may be appreciable in the presence of extremely large fields. A complete vibrational analysis must include consideration of the time dependence of the electromagnetic fields of external and metal origin. Again these effects are expected to be small in the EMIRS and SNIFTIRS experiments.

In addition to these examples, detailed studies have been undertaken on the tetracyanoethylene radical ion system, the hexacyanoferrate system, difluorobenzene adsorption, anthracene adsorption and radical ions, cyanide adsorption, the adsorption of CO and metal-CO and CO/CO interactions, small organic molecule electrocatalytic oxidations at noble metal electrodes, adsorption of nitriles, thiocyanate adsorption, and sulfate/bisulfate adsorption, and the reader is referred to the reviews (4-6) for a complete list of references for those studies.

Vigorous growth in EMIRS and SNIFTIRS has taken place in the last few months, and more sophisticated equipment and experiments are being planned and built. Experiments in the far infrared region (to 50 cm^{-1}) are under way presently in order to study the nature of the metal-adsorbate bond, and other low frequency modes. In addition, extention of work to include single crystal electrodes has already begun; it is felt that those surfaces are required for quantitation of intensity results and a better understanding of the structure

and orientation of adsorbates. Increased sensitivity of these techniques will lead to the _in situ_ study of reactions and dynamics of surface reactions.

Acknowledgements

Literature References

1. H.B. Mark and S. Pons, _Anal. Chem._ 38 (1966) 119.

2. A. Bewick, K. Kunimatsu, and S. Pons, _Electrochim. Acta_ 25 (1979) 465.

3. J.D.E. McIntyre in "Advances in Electrochemistry and Electrochemistry Engineering" Vol. 9, R.H. Mueller, Ed., John Wiley, New York, 1973, p. 61.

4. A. Bewick and S. Pons in "Advances in Infrared and Raman Spectroscopy", R.J.H. Clark and R.E. Hester, Eds., Heyden and Son, London, 1985, in press.

5. S. Pons, A. Bewick, J. Russell, and J. Foley in "Modern Aspects of Electrochemistry", J.O'M. Bockris and E. Yeager, Eds., John Wiley, New York, 1985, in press.

6. A. Bewick and S. Pons, in "Electroanalytical Chemistry", A Bard, Ed., Dekker, New York, 1985, in press.

7. S. Pons, T. Davidson, and A. Bewick, _J. Electroanal. Chem._ 160 (1984) 63.

8. A. Bewick, K. Kunimatsu, S. Pons, and J. Russell, _J. Electroanal. Chem._ 160 (1984) 47.

9. E.U. Condon, _Phys. Rev._ 41 (1932) 759.

10. M.F. Crawford, H.L. Welsh, and J.L. Locke, _Phys. Rev._ 75 (1949) 1607.

11. M.F. Crawford and I.R. Dagg, _Phys. Rev._ 91 (1953) 1569.

12. M.F. Crawford and R.E. MacDonald, _Can. J. Phys._ 36 (1958) 1022.

13. E.D. Palik, R.T. Holm, A. Stella, and H.L. Hughes, _J. Appl. Phys._ 53 (1982) 8454.

14. A. Stella, L. Miglio, E.D. Palik, R.T. Holm, and H.L. Hughes, _Physica_ 117B, 118B (1983) 777.

15. P. Handler and D.E. Aspnes, Phys. Rev. Letters 17 (1966) 1095.

16. R.G. Brewer and A.D. McLean, Phys. Rev. Letters 21 (1968) 271.

17. J.K. Sass, H. Neff, M. Moskovits, and S. Holloway, J. Phys. Chem. 85 (1981) 621.

18. J.P. Devlin and K. Consani, J. Phys. Chem. 85 (1981) 2597.

19. R.E. Hester in "Advances in Infrared and Raman Spectroscopy", Vol. 4, R.J.H. Clark and R.E. Hester, Ed., Heyden and Son, London, 1978, Chapter 1.

20. S. Lehwald, H. Ibach, and J.E. Demuth, Surf. Sci. 78 (1978) 577.

21. S. Pons, S.B. Khoo, A. Bewick, M. Datta, J.J. Smith, S. Hinman, and G. Zachmann, J. Phys. Chem. (1984).

22. S. Pons and A. Bewick, Langmuir, in press.

23. A. Bewick, C. Gibilaro and S. Pons, Langmuir, in press.

24. A. Bewick, S. Pons, and C. Korzeniewski, Electrochim. Acta, in press.

25. I.V. Aleksandrov, Y.S. Bobovich, V.G. Maslovad, and A.N. Siderov, Opt. Spectros. 35 (1973) 154.

26. S. Pons, T. Davidson, and A. Bewick, J. Electroanal. Chem. 140 (1982) 211.

27. P. Saumagne, Ph.D. Thesis, Université de Bordeaux, France, 1981.

28. A. Bewick and A.M. Tuxford, J. Electroanal. Chem. 47, 253 (1973). A. Bewick, K. Kunimatsu, J. Robinson and J.W. Russell, J. Electroanal. Chem. 119 (1981) 175.

29. J.D.E. McIntyre and W.F. Peck, Proc. Symp. Electrocatalysis, The Electrochemical Society, San Francisco, 1974.

30. A. Bewick and J.W. Russell, J. Electroanal. Chem. 132 (1982) 329.

31. A. Bewick and J.W. Russell, J. Electroanal. Chem. 142 (1982) 337.

32. S. Trasatti, J. Electroanal. Chem., in press.

33. A. Bewick, Symposium on the Chemistry and Physics of Electrocatalysis, The Electrochemical Society, San Francisco, (1983).

34. A. Bewick, J. Electroanal. Chem. 150 (1983) 481.

Figure Legends

Figure 1   (a) Internal and (b) external reflection spectroscopy. In (a), an evanescent wave formed at the boundary between the two media penetrates the rarer medium and can interact with absorbers close to the interface.

Figure 2   The relation between electric field strength, angle of incidence, and polarization of radiation with respect to the plane of incidence.

Figure 3   The EMIRS/SNIFTIRS cell.

Figure 4   Difference SNIFTIRS spectrum of benzophenone/ketyl radical.

Figure 5   Difference SNIFTIRS spectrum of TBAF in dry acetonitrile.

Figure 6   Difference SNIFTIRS spectrum of TBAF in wet acetonitrile.

Figure 7   (a) Model of water adsorption at platinum.
(b) Assumed reference state.

Figure 8   EMIRS spectra from $Pt/HClO_4/HCHO$ system, 0 to 250 mV in (a) the absence and (b) the presence of a submonolayer amount of deposited lead.

Figure 9   Difference spectrum of anthracene $A_g\nu_4$ in the strong field region of a polarized electrode.
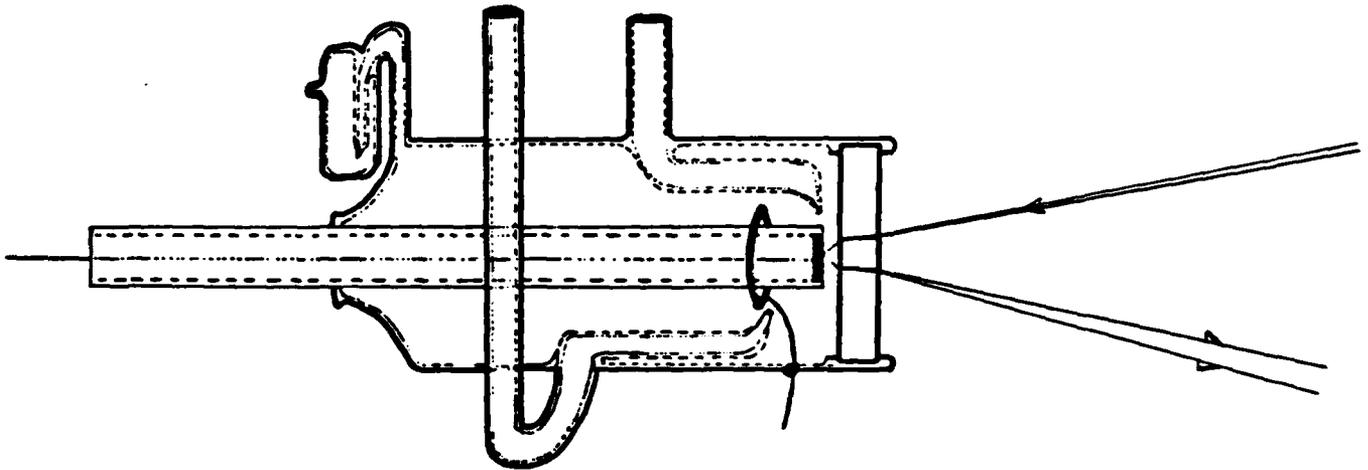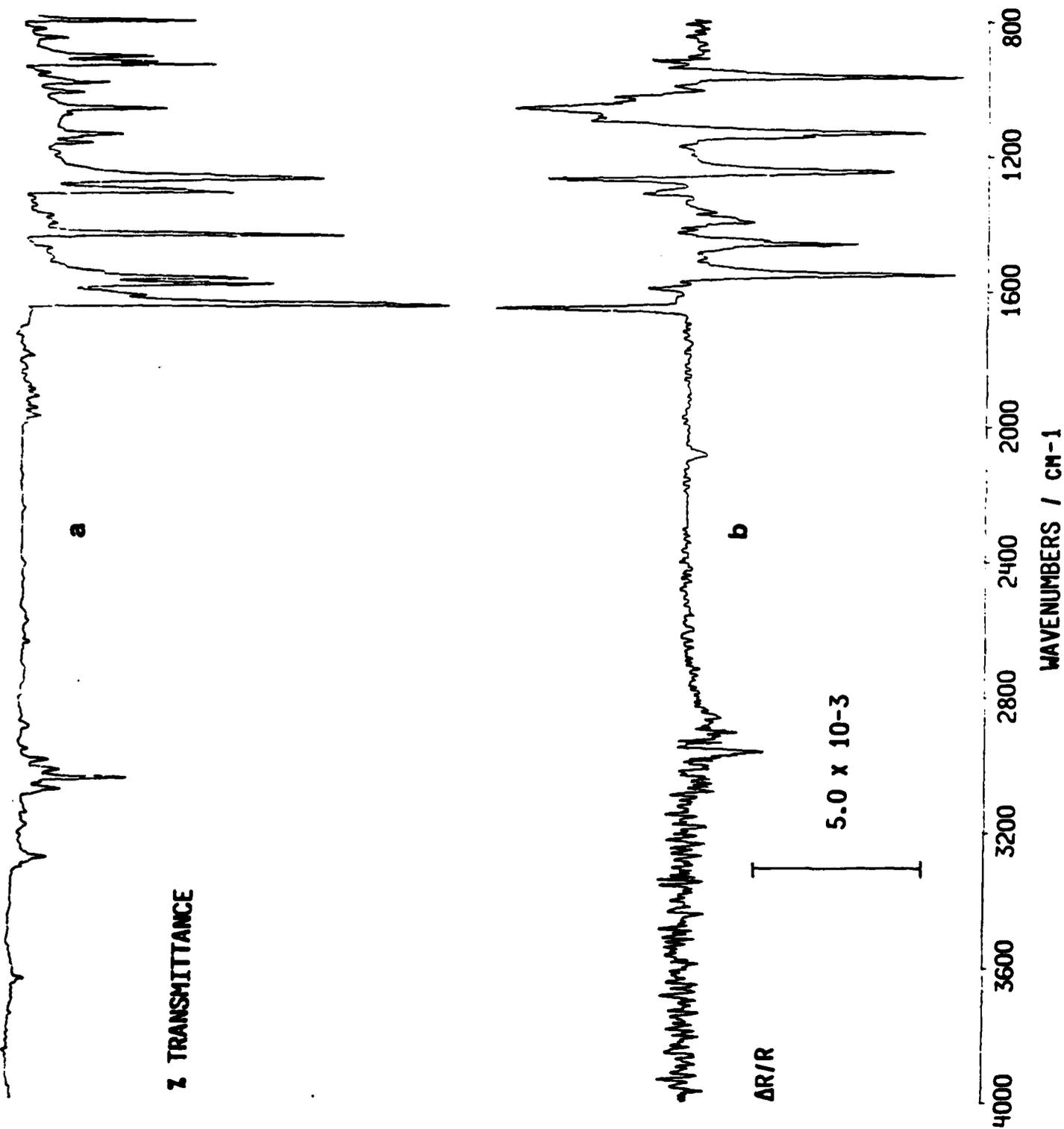
23
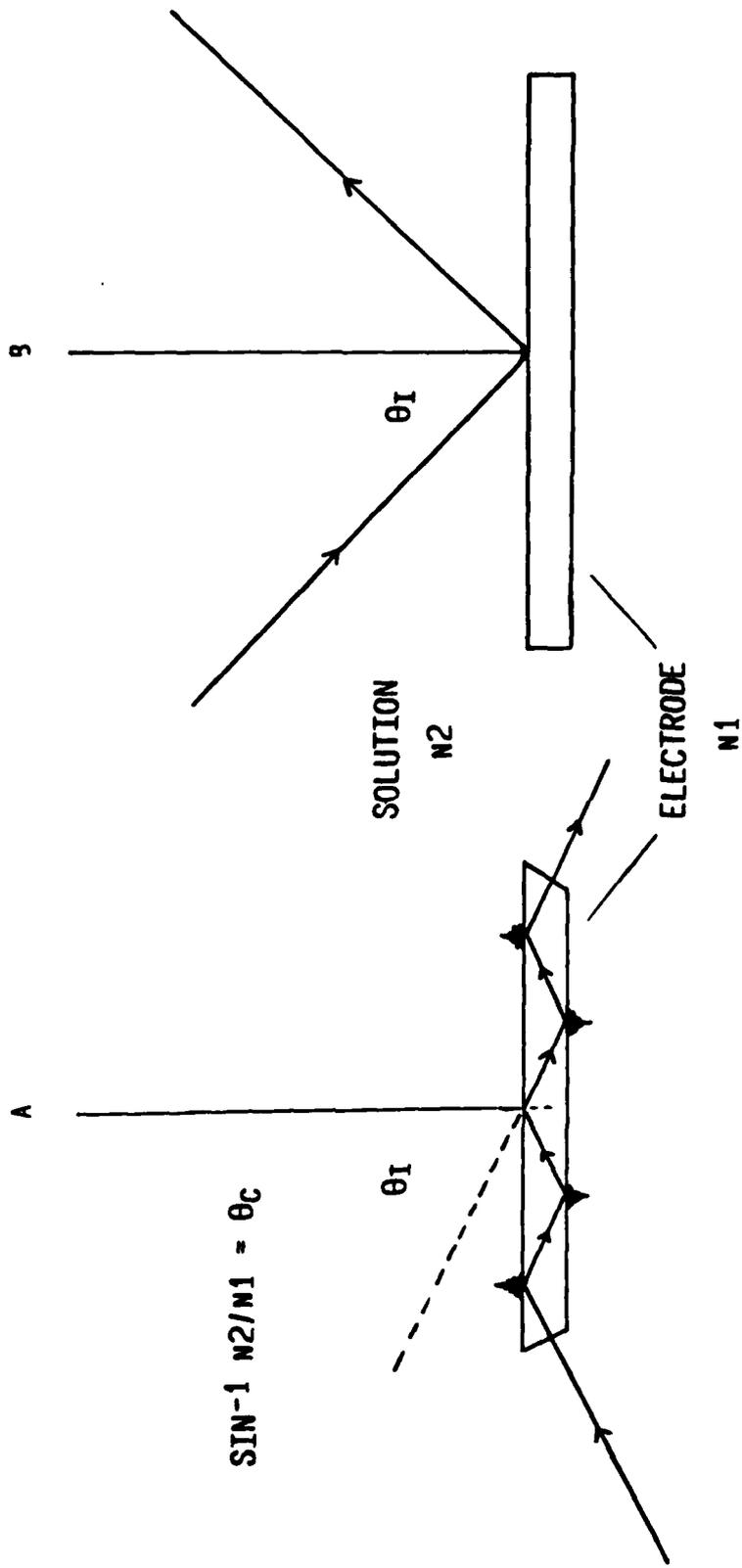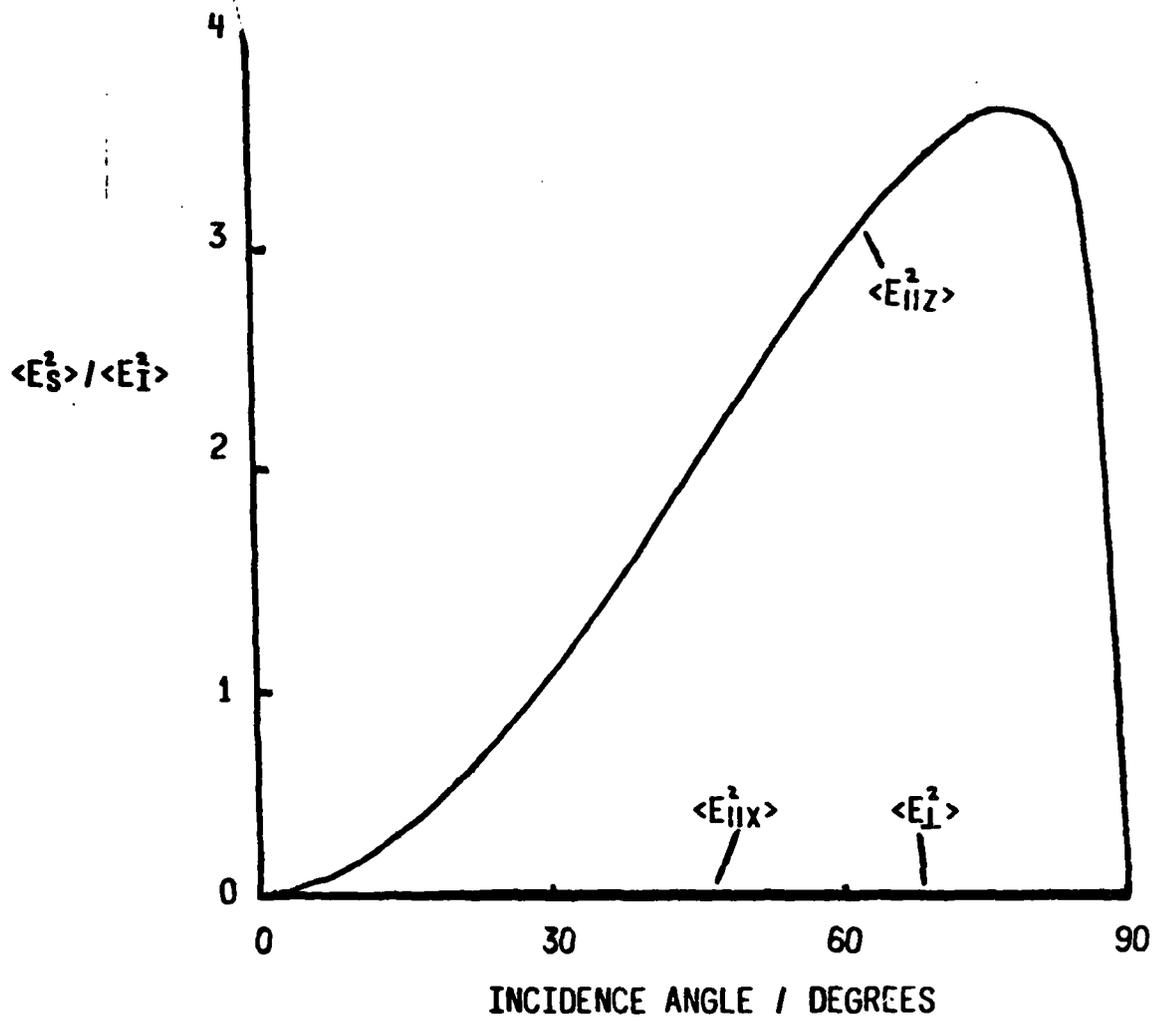
Figure 1

Figure 2

Figure 3

Figure 4

Figure 5

27

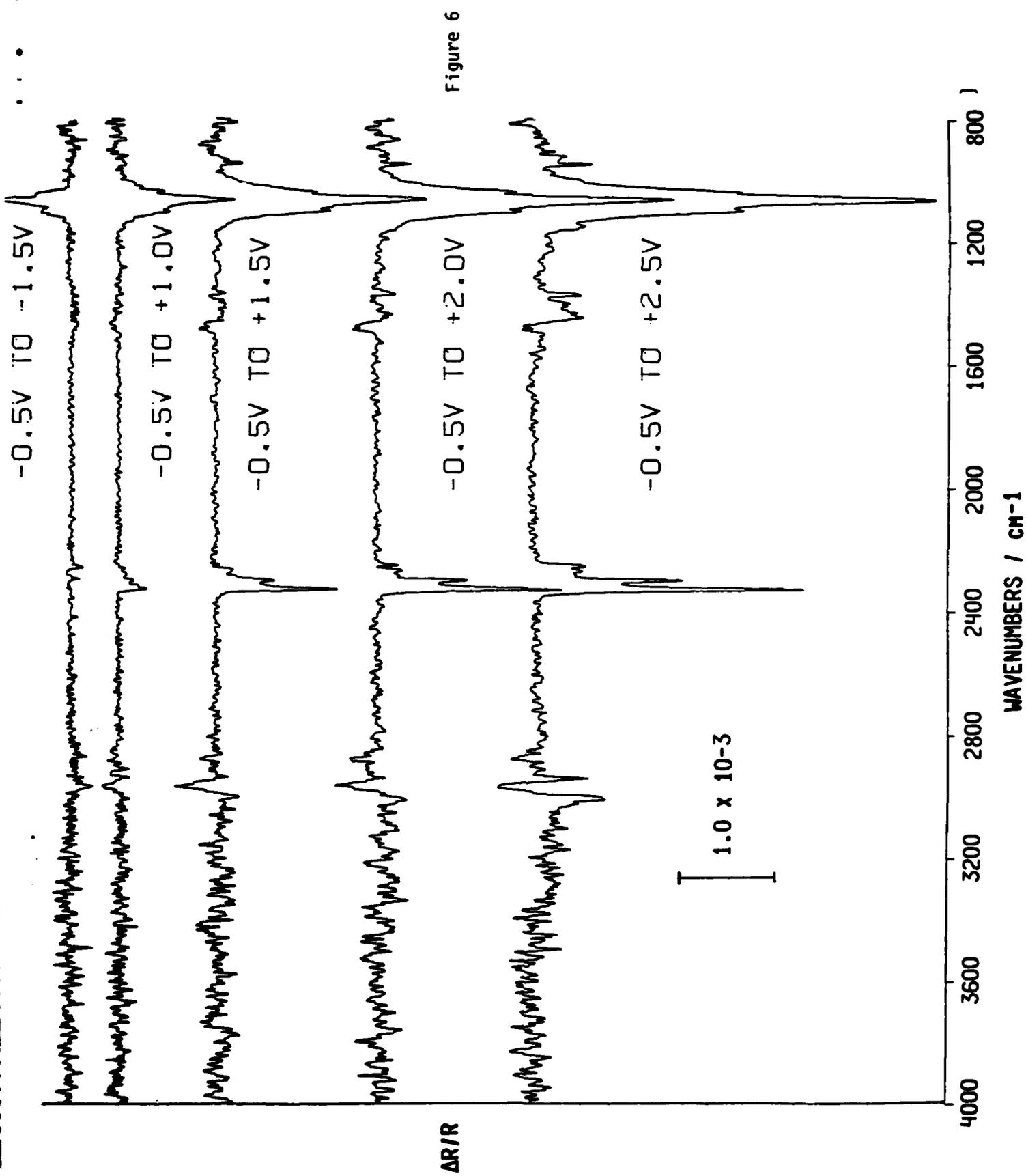$\Delta R/R$

-0.5V TO -2.5V

-0.5V TO +0.5V

-0.5V TO +1.0V

-0.5V TO +1.5V

-0.5V TO +2.0V

-0.5V TO +2.5V

1.0 x 10-3

WAVENUMBERS / CM-1

800   1200   1600   2000   2400   2800   3200   3600   4000

Figure 6

-0.5V TO -1.5V

-0.5V TO +1.0V

-0.5V TO +1.5V

-0.5V TO +2.0V

-0.5V TO +2.5V

1.0 x 10-3

ΔR/R

WAVENUMBERS / CM-1

800   1200   1600   2000   2400   2800   3200   3600   4000

Figure 7

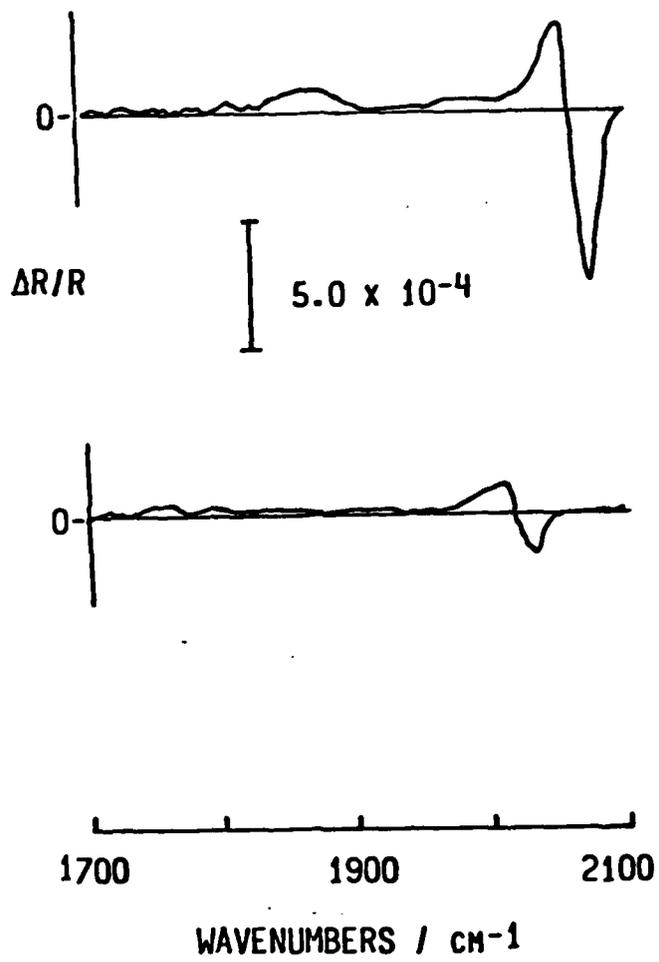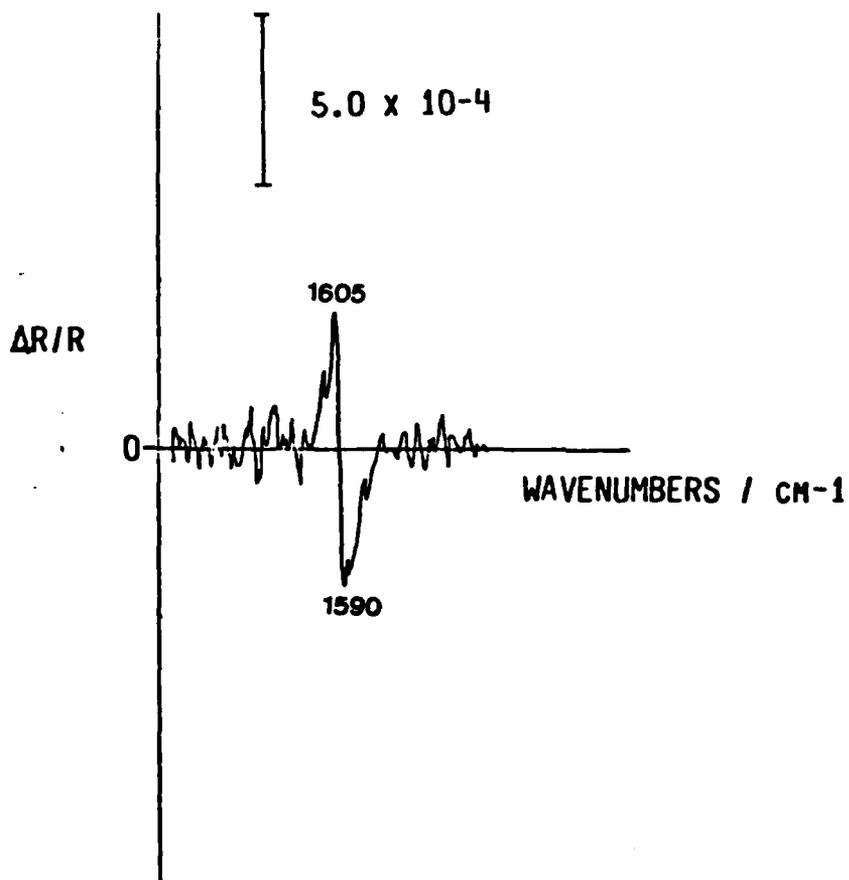$\Delta R/R$ 5.0 x 10^{-4}

1700   1900   2100

WAVENUMBERS / CM^{-1}
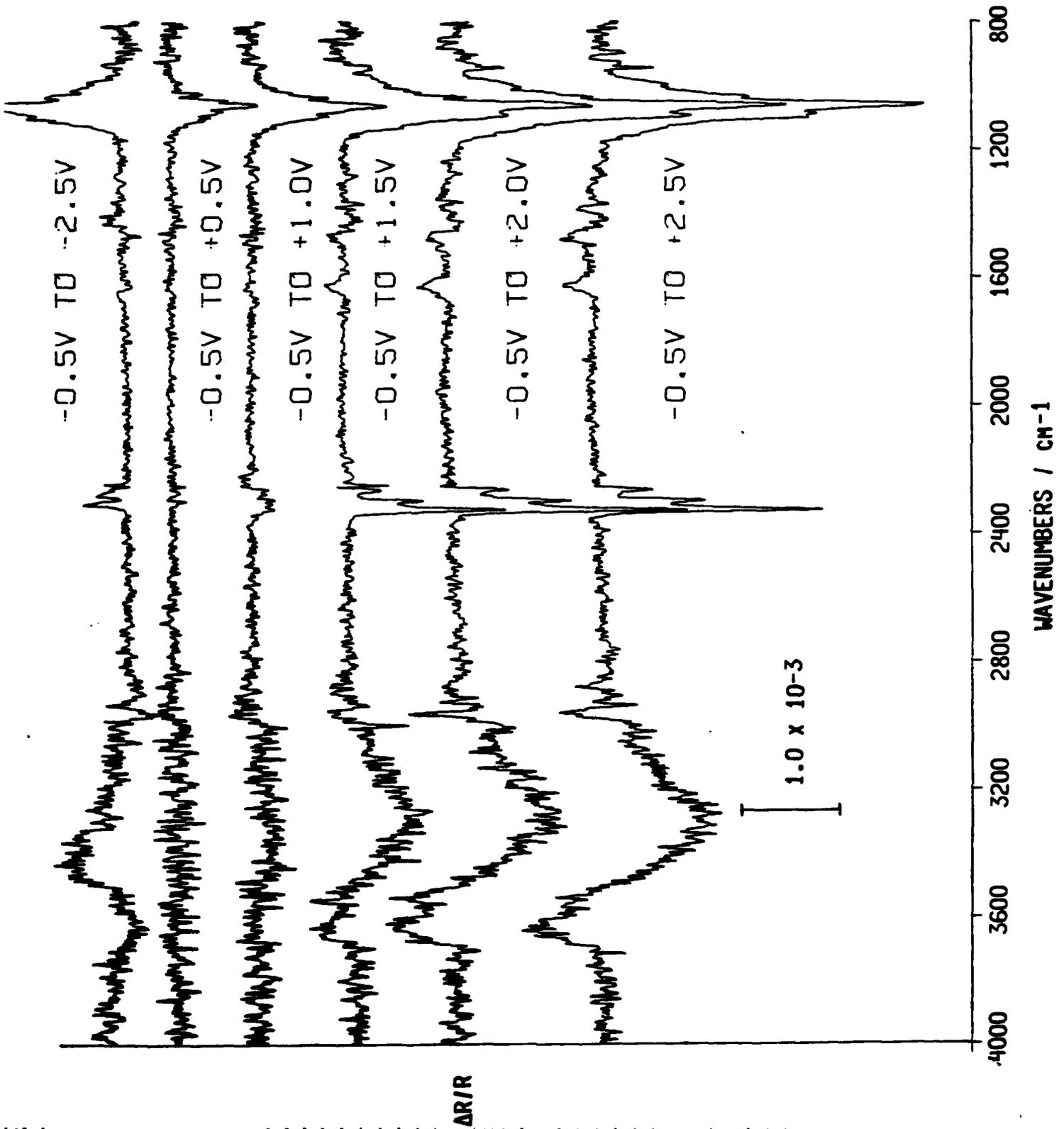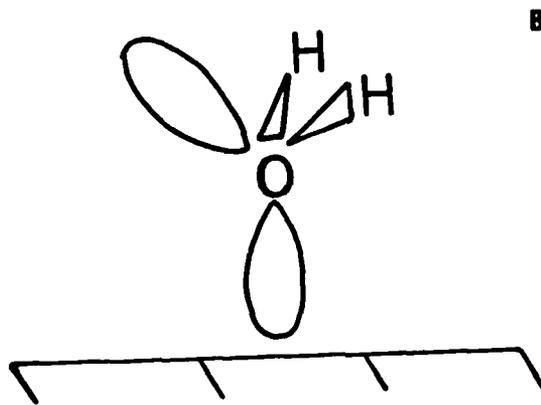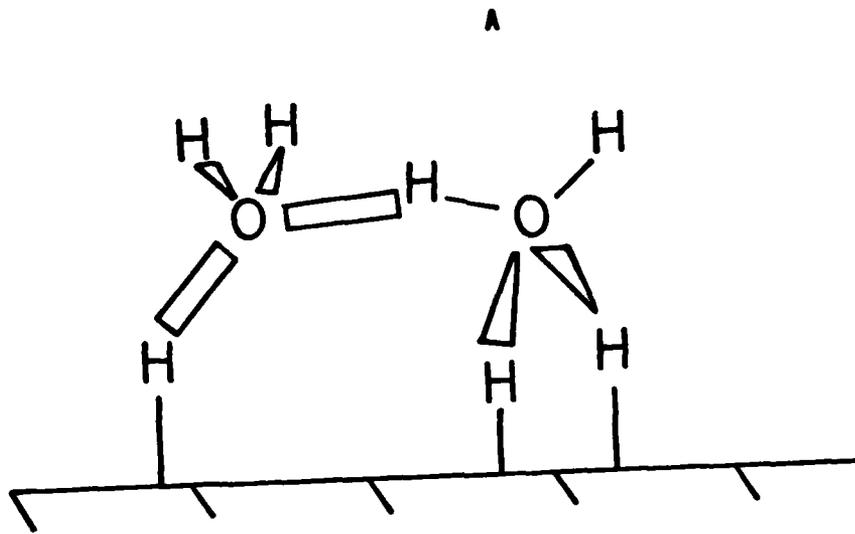
Figure 8

Figure 9

END

FILMED

1-85

DTIC